Targeting eIF5A Hypusination Prevents Anoxic Cell Death through Mitochondrial Silencing and Improves Kidney Transplant Outcome

Nicolas Melis, Isabelle Rubera, Marc Cougnon, Sébastien Giraud, Baharia Mograbi, Amine Belaïd, Didier Pisani, Stephan Huber, Sandra Lacas-Gervais, Konstantina Fragaki, et al.

BASIC RESEARCH www.jasn.org

Targeting eIF5A Hypusination Prevents Anoxic Cell Death through Mitochondrial Silencing and Improves Kidney Transplant Outcome

Nicolas Melis,* Isabelle Rubera,* Marc Cougnon,* Sébastien Giraud,†‡§ Baharia Mograbi,‖ Amine Belaid,‖ Didier F. Pisani,¶ Stephan M. Huber,** Sandra Lacas-Gervais,†† Konstantina Fragaki,‖ Nicolas Blondeau,‡‡ Paul Vigne,¶ Christian Frelin,¶ Thierry Hauet,†‡§ Christophe Duranton,* and Michel Tauc*

*Laboratoire de Physio-Médecine Moléculaire, Centre National de la Recherche Scientifique-UMR7370, ‖Institut de Recherche sur le Cancer, Centre National de la Recherche Scientifique-UMR7284, Institut National de la Santé et de la Recherche Médicale U1081, ¶Institute of Biology Valrose, Centre National de la Recherche Scientifique-UMR7277 Institut National de la Santé et de la Recherche Médicale U1091, ††Centre Commun de Microscopie Appliquée, and ‡‡Institut de Physiologie Moléculaire et Cellulaire, Centre National de la Recherche Scientifique Unité Mixte de Recherche UMR7275, University Nice-Sophia Antipolis, Nice, France; †Centre Hospitalo Universitaire Poitiers, Service de Biochimie, Poitiers, France; ‡Institut National de la Santé et de la Recherche Médicale U1082 Ischémie Reperfusion en Transplantation d'Organes Mécanismes et Innovations Thérapeutiques, Poitiers, France; §Faculté de Médecine et de Pharmacie, Université de Poitiers, Poitiers, France; and **Department of Radiation Oncology, University of Tübingen, Tuebingen, Germany

ABSTRACT

The eukaryotic initiation factor 5A (eIF5A), which is highly conserved throughout evolution, has the unique characteristic of post-translational activation through hypusination. This modification is catalyzed by two enzymatic steps involving deoxyhypusine synthase (DHPS) and deoxyhypusine hydroxylase (DOHH). Notably, eIF5A may be involved in regulating the lifespan of *Drosophila* during long-term hypoxia. Therefore, we investigated the possibility of a link between eIF5A hypusination and cellular resistance to hypoxia/anoxia. Pharmacologic targeting of DHPS by *N*1-guanyl-1,7-diaminoheptane (GC7) or RNA interference–mediated inhibition of DHPS or DOHH induced tolerance to anoxia in immortalized mouse renal proximal cells. Furthermore, GC7 treatment of cells reversibly induced a metabolic shift toward glycolysis as well as mitochondrial remodeling and led to downregulated expression and activity of respiratory chain complexes, features characteristic of mitochondrial silencing. GC7 treatment also attenuated anoxia-induced generation of reactive oxygen species in these cells and in normoxic conditions, decreased the mitochondrial oxygen consumption rate of cultured cells and mice. In rats, intraperitoneal injection of GC7 substantially reduced renal levels of hypusinated eIF5A and protected against ischemia-reperfusion–induced renal injury. Finally, in the preclinical pig kidney transplant model, intravenous injection of GC7 before kidney removal significantly improved graft function recovery and late graft function and reduced interstitial fibrosis after transplant. This unconventional signaling pathway offers an innovative therapeutic target for treating hypoxic-ischemic human diseases and organ transplantation.

J Am Soc Nephrol 28: 811–822, 2017. doi: 10.1681/ASN.2016010012

In transplantation process, ischemia injury is associated with delayed graft function and chronic graft dysfunction; thus, new treatment strategies have to be developed through the highlighting of new pathways involved in ischemic tolerance. For this purpose, we explored the translational machinery that is an essential step involved in the development of physiologic functions and/or progression of diseases[1] and that consumes a great part of the ATP

Received January 6, 2016. Accepted July 20, 2016.

N.M. and I.R. contributed equally to this work. C.D. and M.T. contributed equally to this work.

Published online ahead of print. Publication date available at www.jasn.org.

Correspondence: Dr. Michel Tauc, LP2M, CNRS-7370, 28 Avenue de Valombrose, 06107 Nice Cedex 2, France. Email: michel.tauc@unice.fr

produced by oxidative phosphorylation and oxygen consumption.[2] Translational control is mediated through the selective translation of specific mRNAs, and a limited number of initiation factors is involved in this process. Among these crucial factors, the eukaryotic initiation factor 5A (eIF5A) is highly conserved throughout evolution[3]; its unique characteristic is evident in its activation through hypusination that requires the sequential action of two enzymatic steps catalyzed by deoxyhypusine synthase (DHPS) and deoxyhypusine hydroxylase (DOHH). DHPS transfers the aminobutyl moiety from spermidine to the ε-amino group of a specific lysine residue in the eIF5A precursor protein, whereas DOHH completes hydroxylation to its active functional form.[4] eIF5A is the only protein known to be hypusinated.[5,6] Over the last years, there has been a conceptual evolution concerning the role of eIF5A in the translational mechanism. eIF5A was initially described as a translation initiation factor,[7] but recent studies have shown that eIF5A interacts after the initiation step on translating ribosomes only.[8] Concerning its role at the cell level, the absolute requirement for the eIF5A protein and its post-translational modification was established in yeast[9] and eukaryotic cells[10] proliferation. eIF5A has also been shown to be involved in physiologic processes, such as the HIV replication, the inflammatory state, or the progression of diabetes.[11] However, in the Drosophila model, an interesting role of eIF5A has been highlighted as a potential target for promoting an improvement in the lifespan of flies submitted to low oxygen–containing atmosphere.[12] Because the prevention of the deleterious effects of ischemia is a major challenge in various hypoxic-ischemic–related human diseases, including organ transplantation, the aims of this work were to look for a putative implication of eIF5A in the mechanism underlying mammalian cell death in anoxic conditions and highlight this target in the improvement of kidney transplantation. We chose to use proximal cells from the kidney, a highly oxygen–sensitive organ, and show that inhibition of eIF5A hypusination induced anoxia tolerance through a reversible mitochondrial silencing characterized by a specific downregulation of respiratory chain complexes. We transposed these data to a model of rat ischemic renal stress[13] and evidenced a beneficial effect of *N*1-guanyl-1,7-diaminoheptane (GC7), a highly specific inhibitor[14] of DHPS, in the protection of kidney submitted to ischemia. Finally, we addressed the ischemia-reperfusion injury that surgeons face during organ transplantation. We used the highly relevant model of kidney transplantation in the pig and found that GC7 largely improved the functional recovery of the graft. To evidence the role of eIF5A inhibition in ischemia tolerance, we targeted the DHPS–mediated activation step leading to eIF5A hypusination through the use of both GC7 and siRNA directed against sequences encoding DHPS and DOHH. We show that the pharmacologic inhibition of eIF5A hypusination by GC7 preserves cells from anoxic–induced cell death and can be directly extended to mammals and potentially, humans through its ability to protect the kidney against an ischemia-reperfusion injury. This innovative pharmacologic target of ischemia tolerance paves the way for future fundamental studies, clinical applications, and pharmacologic developments in any physiologic or pathologic situations in which oxygen requirement is crucial.

RESULTS

Inhibition of eIF5A Hypusination Protects Cells from Anoxia–Induced Cell Death

We confirmed that GC7 treatment (30 μM for 24 hours) diminished the ratio of hypusinated eIF5A to total eIF5A in a model of immortalized mouse renal proximal (PCT) cells[15] (Supplemental Figure 1). We next studied the effects of the inhibition of eIF5A hypusination on these PCT cells exposed for 24 hours to normoxia (21% O_2) or anoxia (O_2<0.1%). Under normoxic conditions, GC7 treatment for 24 hours (Figure 1, A and D) or siRNA-mediated silencing of DHPS or DOHH enzymes (Figure 1E, Supplemental Figure 2A) did not affect cell viability (95%± 3% of cells were green labeled and alive). By contrast, a 24-hour period of anoxia markedly decreased the number of green–labeled living cells (8%±2%) concomitantly to an increase in the number of red–labeled dead cells (Figure 1B). Anoxia–induced cell death was largely prevented by (*1*) GC7 treatment in a dose-dependent manner (Figure 1, F and G) with a maximum effect around 30 μM (85%±1% of cells remained viable) (Figure 1, B and D) or (*2*) siRNA targeting DHPS or DOHH enzymes (>80% of cells remained viable) (Figure 1, C and E).

Inhibition of eIF5A Hypusination Induces Metabolic Shift and Mitochondrial Remodeling

GC7 treatment (30 μM for 24 hours) did not modify the intracellular ATP level under normoxic conditions (Figure 2A) but prevented the drop induced by anoxia (O_2<0.1%). The canonical response to anoxia is a downregulation of oxidative phosphorylation accompanied by a metabolic shift toward anerobic glycolysis to ensure the energetic status.[16,17] As shown on Figure 2B, in normoxia, GC7 induced an increase of the basal glucose consumption in a dose-dependent manner, with a maximum effect around 30 μM. This metabolic shift is correlated to the dose-response that we obtained with the live-dead assay (Figure 1, F and G). This glucose consumption increase is significantly enhanced within 3 hours and a maximum of 6 hours after the addition of GC7 (Supplemental Figure 2B) and fully reversible after GC7 removal (Supplemental Figure 2C). We confirmed that this metabolic shift is caused by the inhibition of eIF5A hypusination, because RNAi-mediated knockdown of DOHH enzyme (siRNA) mimicked the increase of glucose consumption induced by GC7 (Supplemental Figure 2D). The cytosolic stabilization of the Hypoxia Induced Factor-1α (HIF-1α) is a classic cell adaptive response to hypoxia.[16] Under normoxia, GC7 did not promote HIF-1α stabilization (Supplemental Figure 3A). By contrast, anoxia induced a marked increase in HIF-1α levels in both the presence and absence of GC7. These results suggest

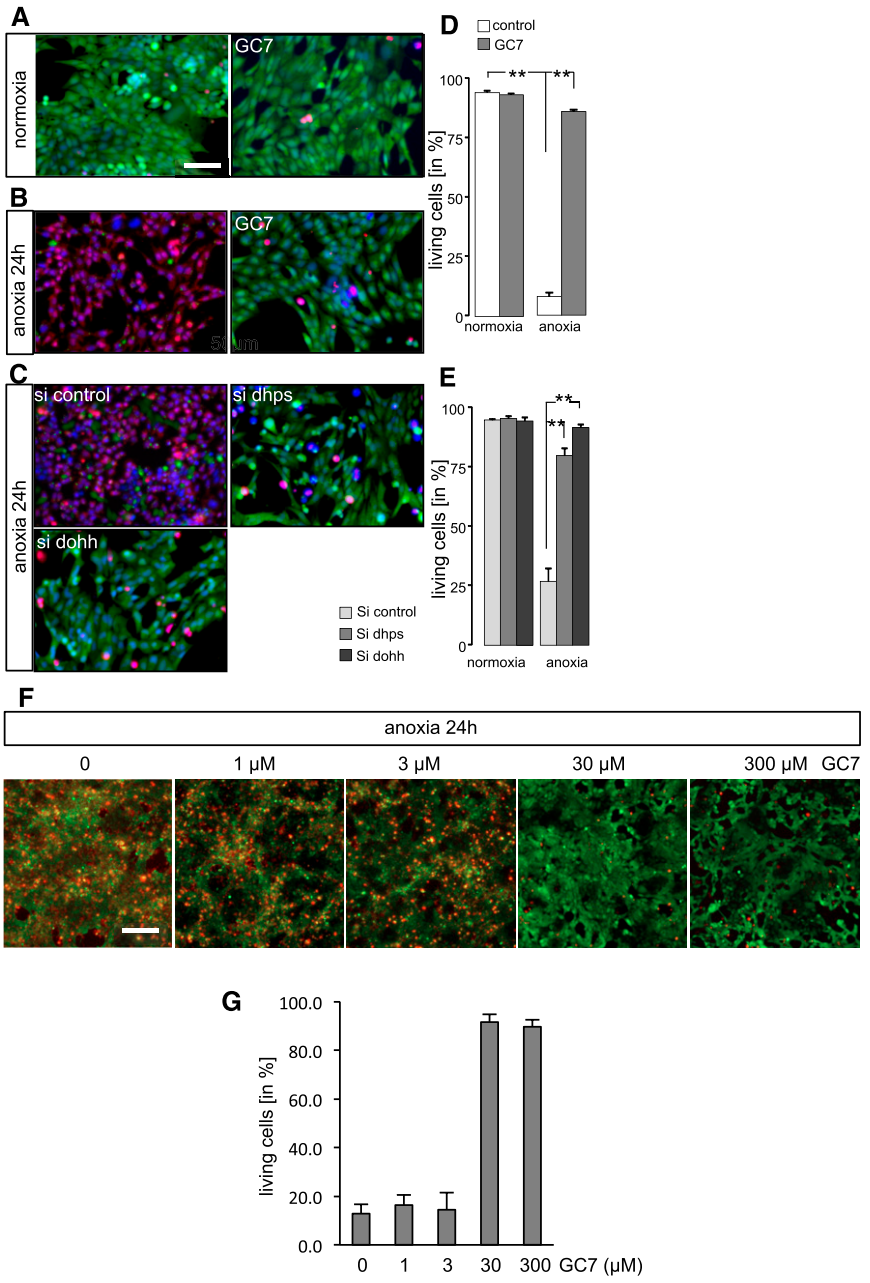

Figure 1. Inhibition of eIF5A hypusination prevents anoxia–induced cell death. (A and B) Representative images of renal PCT cells exposed to (A) normoxia (20% O_2) or (B) anoxia (24 hours of O_2<0.1%) in the presence or absence of 30 μM GC7. Living cells are green labeled (calcein-AM), dead cells are red labeled (homodimeric BET), and nuclei are blue labeled (DAPI). Scale bar, 50 μm. (A) GC7 treatment (30 μM) and (C) mRNA silencing (siRNA) of DOHH or DHPS significantly reduced cell death induced by anoxia. Control siRNA (scrambled sequence) remained without effect. (D and E) Quantification of cell viability from A–C. (F) Micrographs of subconfluent PCT cells maintained in anoxic conditions for 24 hours in the presence of various concentrations of GC7. Scale bar, 100 μm. (G) The live-dead assay was used to determine the rate of cell death that is shown on the histogram. Data are means±SEM for 600 cells per well of triplicate samples per condition. **P<0.01, one-way ANOVA. O_2, oxygen.

that GC7 induces a reversible metabolic shift toward glycolysis and promotes anoxic tolerance in an HIF-1α–independent manner. Because a metabolic shift is often correlated with a change in oxidative phosphorylation, we looked for the effect of GC7 on mitochondrial potential using the $\Delta\Psi_m$-sensitive fluorescent dye TMRE and FACS analysis. GC7 treatment (30 μM for 24 hours) induced a dose-dependent decrease in fluorescence, reflecting a shift of $\Delta\Psi_m$ toward less negative values (Figure 2, C and D). Interestingly, GC7 never induced a total breakdown of $\Delta\Psi_m$, which was classically observed in cells entering apoptosis (total $\Delta\Psi_m$ dissipation is <3% of the GC7-treated cells only; area M1) (Figure 2C). We obtained the

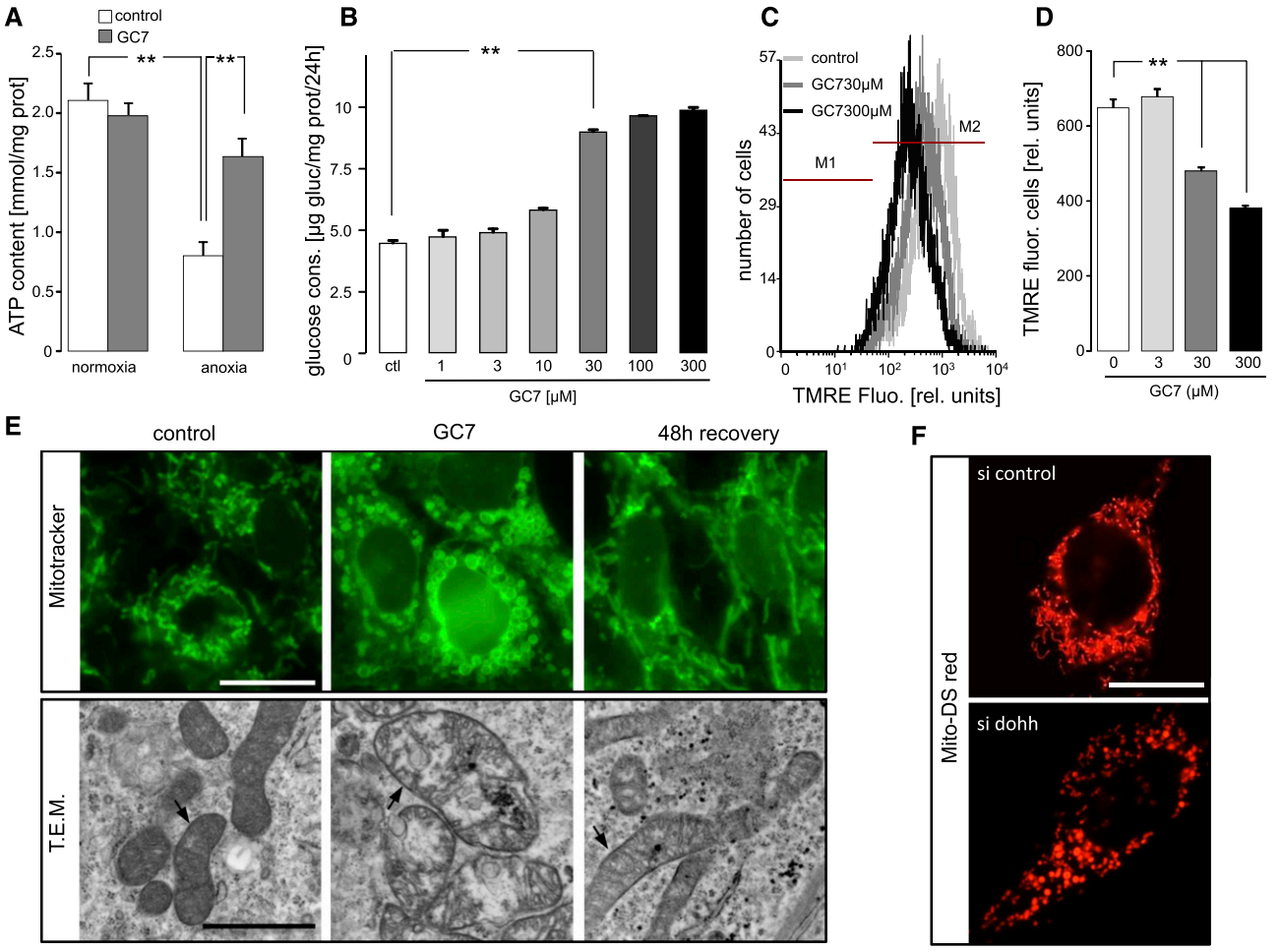

Figure 2. Inhibition of eIF5A hypusination induces mitochondrial remodeling. (A) Intracellular ATP content measured in control and GC7-treated cells exposed to normoxia or anoxia (O_2<0.1% for 24 hours). Values are expressed as means±SEM (n=6). **P<0.01, one-way ANOVA. (B) Glucose consumption in control and GC7–treated PCT cells (1–300 μM) maintained for 24 hours in normoxic atmosphere (20% O_2). Values are means±SEM (n=10–15). **P<0.01, one-way ANOVA. Distribution of (C) mitochondrial $\Delta\Psi_m$ and (D) related geometric means measured in PCT cells exposed to various GC7 concentrations. Cells were loaded with the $\Delta\Psi_m$–sensitive fluorescent dye TMRE and analyzed by flow cytometry. Values are expressed as means±SEM (n=6). **P<0.01, one-way ANOVA. (E) Mitochondrial network organization observed in control and GC7–treated PCT cells (30 μM for 24 hours) and after 48 hours recovery using MitoTracker Green FM labeling. Scale bar, 20 μm. Representative electron microscopy picture showing mitochondria (arrows) visualized in control and GC7–treated cells (30 μM for 24 hours) and after 48 hours of recovery. Scale bar, 2 μm. (F) Representative micrographs of mitochondrial network organization obtained after 48 hours of transfection with control siRNA (scrambled sequence) and DOHH siRNA. The MitoDSred vector was cotransfected to visualize mitochondria. O_2, oxygen.

same effect by measuring directly the fluorescence of the mitochondrial potential probe Mitotracker red FM[18] on intact confluent epithelia (Supplemental Figure 4). Interestingly, this GC7-induced decrease in $\Delta\Psi_m$ was not related to an upregulation of the uncoupling proteins UCP2 (Supplemental Figure 3B) or UCP3 (Supplemental Figure 3C). GC7 treatment (30 μM for 24 hours) generated a reorganization of the mitochondrial network, which appeared disorganized, with a loss in the tubular continuum profile observed in control cells (Figure 2E). Electron microscopy observations confirmed the GC7-mediated remodeling of the mitochondria; they appeared swollen, with the matrix becoming paler and inhomogeneous, and the cristae were disoriented and reduced in number (Figure 2E). The GC7-mediated modifications of the mitochondrial network and ultrastructure were reversible within 48 hours after drug withdrawal (Figure 2E). Interestingly, targeting DOHH enzyme activity through RNAi-mediated knockdown (siRNA DOHH) mimicked the mitochondrial morphologic modification observed in GC7-treated cells (Figure 2F).

Inhibition of eIF5A Hypusination Induces Functional Subexpression of OXPHOS Mitochondrial Complexes

We evaluated the molecular status of the respiratory chain using antibodies raised against subunits of the OXPHOS

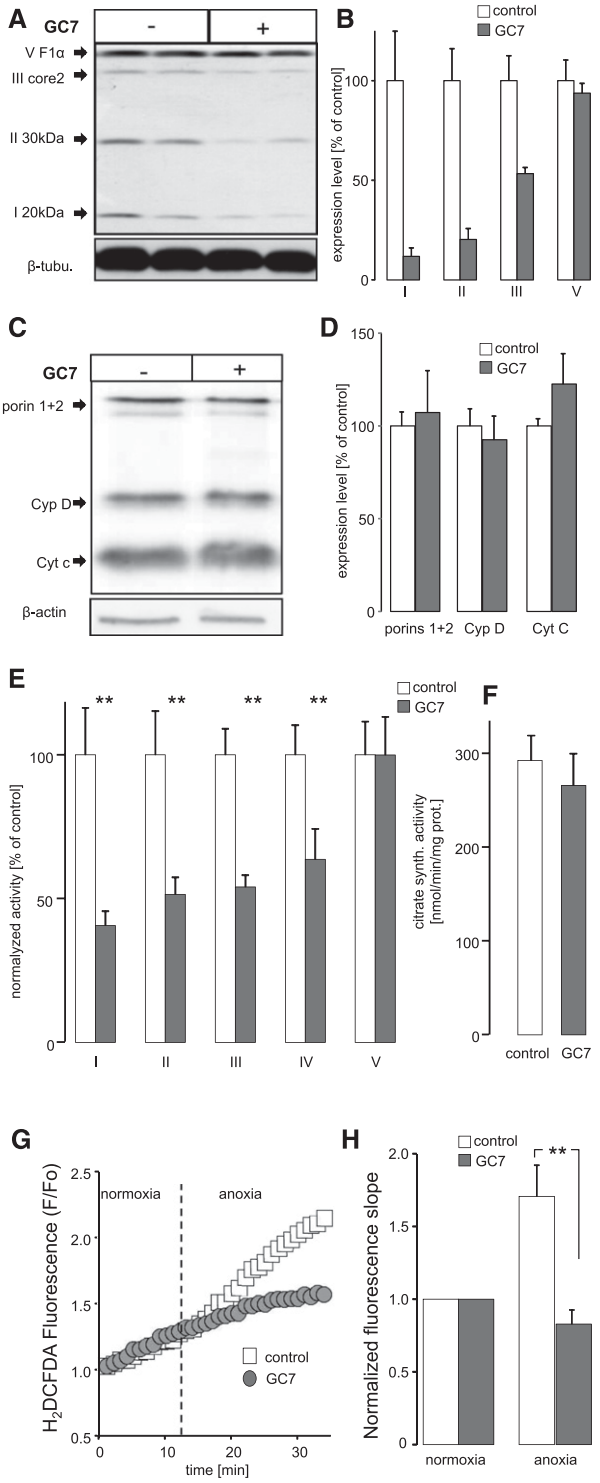

Figure 3. GC7 induces a mitochondrial silencing. (A) Western blotting and (B) related quantitative analysis of complexes (1–3 and 5) subunits expression obtained from control and GC7–treated PCT cells (30 μM for 24 hours). Values are expressed as means±SEM (n=3); β-tubulin was used as an equal loading control. (C) Western blotting and (D) quantitative analysis performed using antibodies raised against the outer mitochondrial membrane proteins (porin 1+2 isoforms), the matrix space (cyclophilin D [Cyp D]), and the intermembrane space (cytochrome C [Cyt C]) in control and GC7–treated PCT cells (30 μM for 24 hours). Values are expressed as means±SEM (n=3); β-actin was used as an equal loading control. Enzymatic activities in percentage of control of (E) mitochondrial complexes 1–5 and (F) citrate synthase obtained from control and GC7–treated PCT cells (30 μM for 24 hours). (G) Time course and (H) mean slope of intracellular ROS accumulation measured in control and GC7-treated cells (30 μM for 24 hours). The atmosphere was shifted from normoxia to anoxia at the indicated time. Values are expressed as the means±SEM (n=4–10). **P<0.01, t test.

complexes and specific proteins of mitochondrial compartments. Expression of complexes 1–3 was significantly decreased in GC7-treated cells (Figure 3, A and B). By contrast, the expressions of other proteins of mitochondrial compartments (porins, cyclophilin D, cytochrome C, and complex 5) remained unaffected (Figure 3, C and D). A significant reduction of mitochondrial complexes 1–4 activity was also observed in GC7-treated cells (Figure 3E). By contrast, complex 5 and citrate synthase activities (a hallmark of the mitochondrial matrix integrity) were not altered (Figure 3, E and F). GC7 induced a drastic reduction in OXPHOS mitochondrial activity through a selective reduction in the expression and the activity of respiratory chain complexes, reflecting a mitochondrial functional silencing.

This unique mitochondrial status induced by GC7 exposure might support the hypothesis of a fall in mitochondrial reactive oxygen species (ROS) generation triggered by anoxia. We measured the time course of ROS formation along with the application of an anoxic stress (O_2<0.1%) (Figure 3G). The fluorescence emitted by the ROS–sensitive probe 5(and 6)-carboxy-2′,7′-dichlorodihydrofluorescein diacetate increased soon after the induction of anoxia in control cells but remained constant in GC7-treated cells (Figure 3, G and H), suggesting that GC7 abolishes anoxia–induced ROS production and protects the cells from the harmful effects of free O_2 radicals.

Inhibition of eIF5A Hypusination Decreases Oxygen Consumption

Polarographic experiments showed that the cellular O_2 consumption measured in PCT cells under normoxia was mainly caused by mitochondrial respiration, displaying (*1*) high sensitivity to the cytochrome poison KCN that specifically inhibits mitochondrial respiration and (*2*) stimulation by the FCCP uncoupler that allows the measurement of maximal mitochondrial O_2 consumption (Figure 4, A and B). GC7 (30 μM for 24 hours) caused a marked time–dependent inhibition in O_2 consumption, reaching 70%, whereas acute exposure had no effect (Figure 4A, Supplemental Figure 5). Cessation of GC7 treatment restored O_2 consumption to near control values within 48 hours (Figure 4B). We next established the bioenergetic profile (Seahorse) of GC7–treated PCT cells. In control cells, the oxygen consumption rate (OCR) was characteristic of a

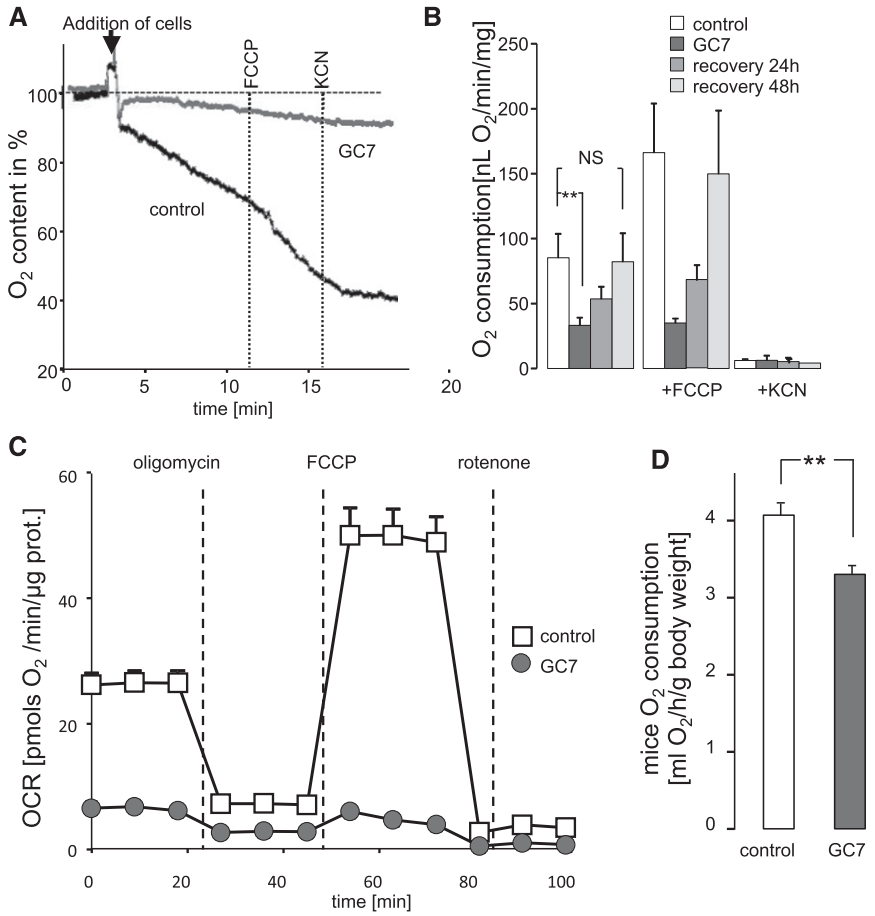

Figure 4. GC7 induces a fall in cellular oxygen consumption. (A) Oxygen consumption as a function of time in control and GC7-treated cells. Cells were successively exposed to the uncoupler FCCP and the inhibitor of OXPHOS, KCN. (B) Means of oxygen consumption measured as in A and after a 24- or 48-hour recovery period without GC7. Values are expressed as means±SEM (n=3–15) **P≤0.01, one-way ANOVA. (C) Bioenergetic profile of control and GC7-treated cells. OCR changes are plotted against time during the Seahorse flux analyzer run. Oligomycin, FCCP, and rotenone were sequentially delivered at the indicated times. OCR values are expressed as the means±SEM (n=11). **P<0.01, one-way ANOVA. (D) Histogram of oxygen consumption measured in control mice (saline solution treated) and GC7-treated mice (daily intraperitoneal injections for 3 days of 3 mg/kg each). Values are means±SEM (n=5). **P<0.01, t test.

bioenergetic profile primarily dedicated to ATP synthesis through oxidative phosphorylation (Figure 4C). GC7 treatment reduced the basal OCR by 80%, and the addition of FCCP had almost no effect on OCR, suggesting that the GC7-treated cells already exhibited the maximal respiratory rate under basal conditions. These results show a drastic reduction in OXPHOS mitochondrial activity and support the previously observed GC7–induced metabolic shift toward glycolysis. This fall in O_2 consumption was also observed *in vivo* after GC7 treatment: an approximately 20% decrease in O_2 consumption was observed in GC7–treated awake mice (3 mg/kg for 24 hours) (Figure 4D) compared with in control mice (details in Concise Methods).

Inhibition of eIF5A Hypusination Protects Kidney against an Ischemic Stress

To explore the role of eIF5A hypusination inhibition during an ischemic stress, we turned to a classic rat model of controlled renal ischemic injury.[13] Adult rats were treated by intraperitoneal GC7 injection (daily injections for 3 days) to evaluate *in vivo* its effect on eIF5A hypusination. This treatment significantly reduced the level of the hypusinated form of eIF5A in the kidney (Figure 5A) in a dose-dependent manner (Figure 5B) without modifying basic physiologic parameters or renal function (Supplemental Table 1). The dose of 3 mg/kg was used to obtain a GC7 concentration comparable with the one used in *in vitro* assays assuming an extracellular space volume of 30%.[19] We induced an unilateral left renal artery ischemia (40 minutes) in rats treated or not treated with GC7 and monitored the related renal functional injury 24 hours later. Renal injury was assessed by (*1*) quantification of urinary neutrophil gelatinase–associated lipocalin (NGAL), an early biomarker of tubular injury[20] and (*2*) measurement of the glucose, Na^+, and PO_4^{3-} fractional excretions (FEs) from the ischemic (left) kidney compared with those obtained from the contralateral control (right) kidney.[21] The urinary NGAL concentrations of the left ischemic kidney significantly increased 24 hours

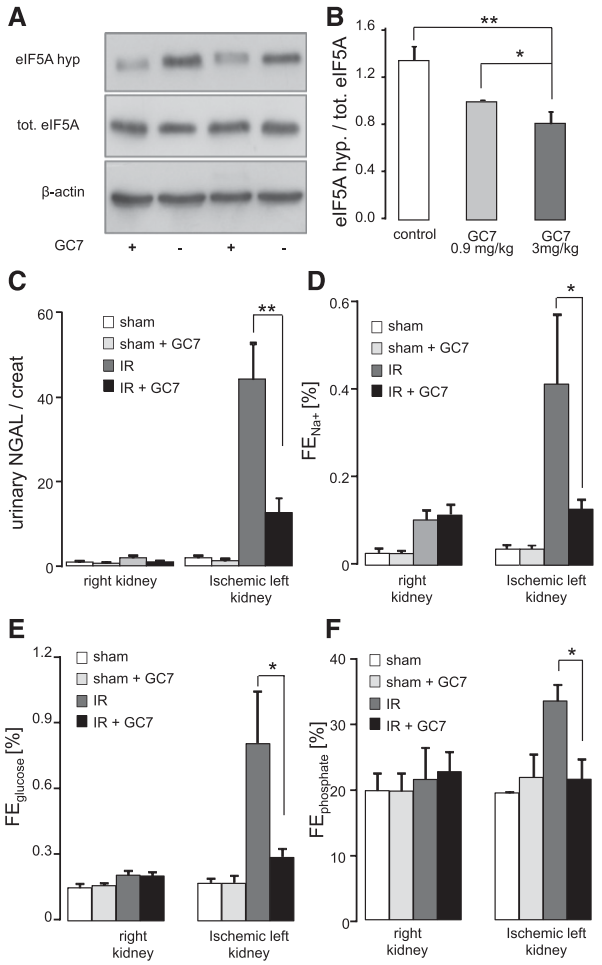

Figure 5. GC7 inhibits eIF5A hypusination in the kidney and protects rats against ischemia-reperfusion–induced renal injury. (A) Western blot of kidney extracts revealed with antibodies raised against the hypusinated and the total form of eIF5A. β-Actin was used as a loading control. (B) Histogram obtained from A showing the hypusinated eIF5A-to-total eIF5A ratio in rats treated with the indicated dose of GC7 (mean±SEM of four rats per group). (C) Urinary NGAL-to-creatinine ratio and FEs of (D) sodium, (E) glucose, and (F) PO_4^{3-} measured in urine from the left ischemic kidney and the right control kidney from sham (sham), GC7–treated sham (sham + GC7), ischemic (IR), and ischemic GC7–treated (IR + GC7) rats 24 hours after ischemia-reperfusion. Values are expressed as means±SEM of 10–18 rats per group. *$P<0.05$, *t* test; **$P<0.01$, *t* test.

after the application of the ischemia-reperfusion protocol (Figure 5C) together with an increase in sodium (Figure 5D), glucose (Figure 5E), and phosphate (Figure 5F) FEs. GC7 treatment prevented the increase in urine levels of NGAL 24 hours after the ischemia-reperfusion protocol (Figure 5C). Furthermore, GC7 largely protected the proximal tubular functions, because the FEs of glucose, PO_4^{3-}, and Na^+ remained similar to those observed in the control nonischemic kidney (Figure 5, D and F). This *in vivo* study shows that inhibition of eIF5A hypusination protects renal function from oxygen deprivation in a model of renal ischemia-reperfusion injury. We next evaluated the effect of GC7 when perfused to the rats after the ischemic injury to determine if it could be used in a post-treatment protocol. In this context and our experimental conditions, we were unable to show a protective effect of GC7 on sodium, glucose, and phosphate FEs (Supplemental Figure 6).

GC7 Improves Kidney Graft Function Recovery and Decreases Fibrosis in a Highly Relevant Preclinical Model of Kidney Transplantation

We tested the relevance of our new concept in a pertinent preclinical porcine model of kidney autotransplantation close to human conditions. We measured the plasma creatinine up to 90 days after kidney transplantation. Figure 6, A and B shows that the ischemia-reperfusion injury alone induces early and late graft dysfunctions. GC7 administration through two successive intravenous injections 24 and 3 hours before pig kidney removal improves significantly the graft function recovery and the late graft function as creatininemia (Figure 6, A and B), sodium FE, osmolarity plasma/urine, alanine aminopeptidase excretion, and plasma aspartate aminoransferase level measurements (Table 1). We also evaluated the diuresis recovery along time, one of the major challenges in kidney transplantation. All GC7–treated animals exhibited an early recovery of diuresis, whereas it lasted 3 days to be effective in vehicle-treated pigs. We looked for the morphologic aspect of the cortical area by electron microscopy on kidney graft biopsies obtained 30 minutes after reperfusion (Figure 6D). In the vehicle group, proximal tubule cells present an altered cytoplasm (low density) with vacuoles, and mitochondria have a relatively good morphology. Microvilli of the brush border appear short, not tight, and edematized. In the GC7-treated group, proximal tubule cells present a dense cytoplasm with few vacuoles and mitochondria with a correct morphology. GC7 clearly improves the morphologic integrity of the kidney brush border. Additionally, the rate of apoptotic cells measured by the terminal deoxynucleotidyl transferase–mediated digoxigenin-deoxyuridine nick end labeling (TUNEL) technique was trend lower in GC7-treated animals (Figure 6E). We evaluated the oxidative stress on these biopsies. The use of GC7 before ischemia permits a significant decrease in the staining of the fluorogenic ROS sensor CellROX (Figure 6F) and a diminution of the lipid peroxidation visualized by 4-HNE labeling (Figure 6G) compared with in the nontreated vehicle group. Thus, GC7 lowers the oxidative stress. To determine the effect of graft treatment with GC7 on chronic fibrosis, we evaluated the degree of interstitial collagen deposition using Sirius red staining[22] (Figure 6H). Treatment with GC7 protects efficiently against the development of chronic interstitial fibrosis 3 months post-transplantation (Figure 6I). The deposition of fibrin in the small vessels and capillaries of the graft is a critical element in the development of chronic kidney fibrosis. Analysis of the expression of tissue plasminogen activator (tPA), an enhancer of fibrinolysis and thus,

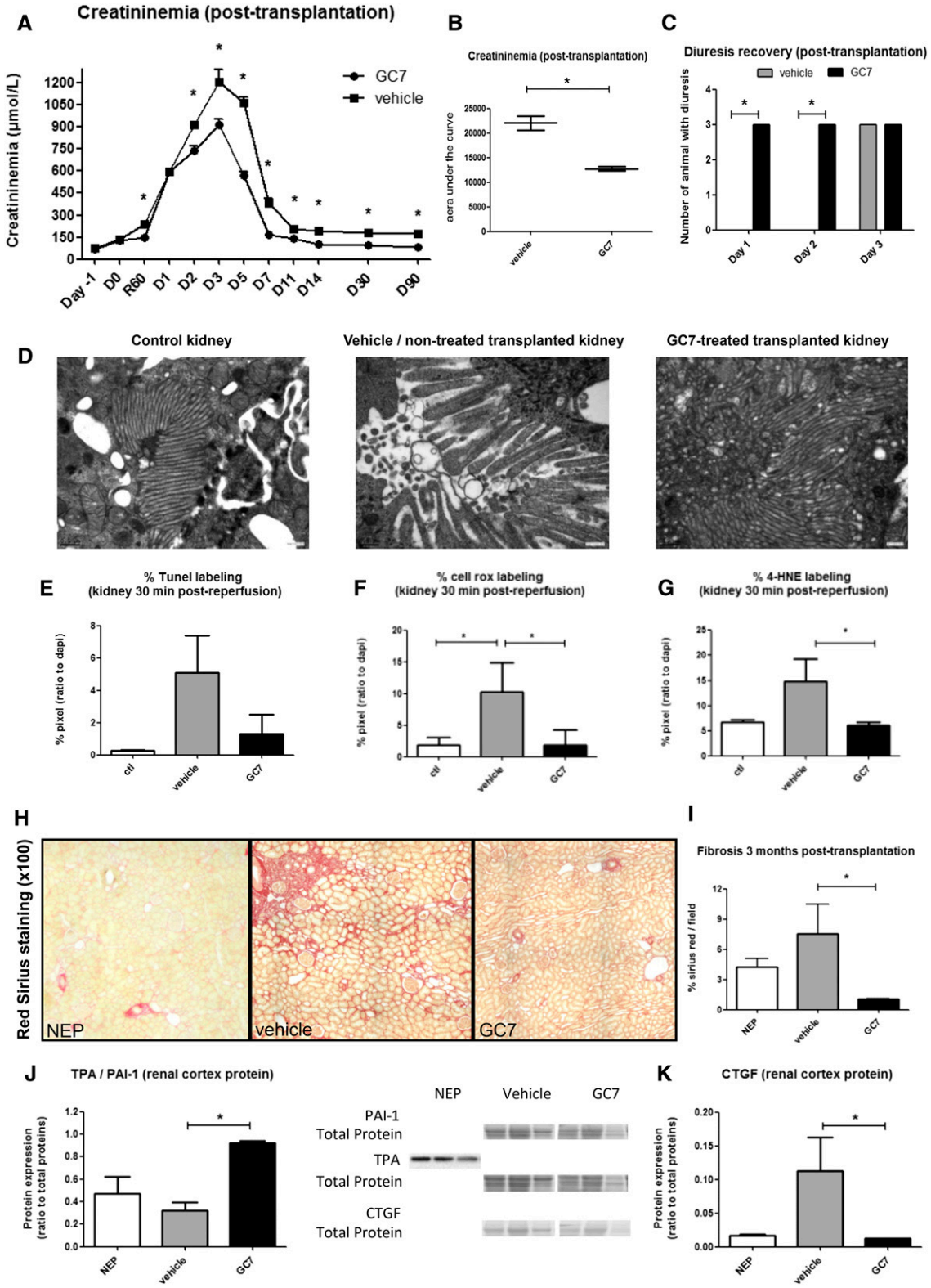

Figure 6. GC7 improves the functional recovery of kidney graft after transplantation in pig. Postreperfusion plasma creatinine levels (A) quantified from day −1 before transplantation to day 90 after kidney transplantation and (B) expressed as area under the curve from day 0 to day 90 after kidney transplantation in vehicle and GC7-treated groups (vehicle is the unilateral nephrectomy control). *$P<0.05$ vehicle versus GC7 group at each time, Mann–Whitney test. (C) Number of animals with diuresis recovery at post-transplantation days 1–3. (D) Electron microscopy of renal biopsies obtained 30 minutes after reperfusion of the nontreated group (vehicle) or the

Table 1. Renal function parameters and injury markers measured in vehicle– and GC7–treated porcine groups (mean±SEM; *n*=3 per group; statistics $P<0.05$ vehicle versus GC7 group were performed with Mann–Whitney test on NCSS software)

Parameters	Vehicle	GC7	Mann–Whitney Test
Sodium FE (area under the curve; from day −1 to day 90 post-transplantation)	440±16.5	324±10	$P<0.05$
Osmolarity plasma/urine (area under the curve; from day −1 to day 90 post-transplantation)	71±0.4	48.5±1	$P<0.05$
Alanine aminopeptidase urine (day 3 post-transplantation), IU/L	256±6	27±2	$P<0.05$
ASAT at 60 min post-transplantation, IU/L	134±5	56±3	$P<0.05$
ASAT at day 1 post-transplantation, IU/L	184±2	106±3	$P<0.05$
ASAT at day 2 post-transplantation, IU/L	71±2	40±3	$P<0.05$
ASAT at day 3 post-transplantation, IU/L	54±1.5	44±3	$P<0.05$
ASAT (area under the curve; from day −1 to day 3 post-transplantation)	375±2	220±6	$P<0.05$

ASAT, aspartate aminotransferase.

protective of the graft, revealed that the protein was critically suppressed in grafts of the vehicle group, whereas it was preserved in the GC7 group. Moreover, we found that PAI-1, inhibitor of tPA,[23] was overexpressed in the vehicle group, whereas it was decreased in grafts treated with GC7 (Figure 6J). We, thus, show that GC7 exposure has a long–term protective effect on the graft against the inhibition of fibrinolysis in the vessels known to promote fibrosis. We also show that the expression of the fibrosis–related factor[24] connective tissue growth factor (CTGF) was suppressed in the GC7-treated group (Figure 6K).

DISCUSSION

The highly conserved factor eIF5A in its hypusinated active form has been already implicated in many cellular, physiologic, and pathologic functions[25–28]; thus, there is a considerable interest in this factor as a potential target for drug development through inhibition of hypusination. More interestingly, a previous work[12] suggested that eIF5A could be associated with the survival rate of flies maintained in hypoxic atmosphere. Because this last result could be of high relevance in human ischemic diseases, we investigated the putative involvement of eIF5A in an ischemic–related kidney disease. Impairment of proximal tubules by ischemia is one of the most frequent causes of renal failure.[29] This sensitivity toward oxygen deprivation is because of their highly aerobic metabolism associated with a poor capacity of regeneration.

Using cultured immortalized proximal cells, we showed an unsuspected link between eIF5A hypusination status and mitochondrial respiratory chain complexes expression, ROS production, O_2 consumption, and resistance to hypoxic-anoxic situations. We used the spermidine analog[3] GC7 that is a competitive inhibitor exhibiting a K_i of 10 nM toward DHPS *in vitro*.[14] We confirmed DHPS as the target of GC7 through an siRNA strategy silencing the enzymes (DHPS and DOHH) in charge of eIF5A hypusination. Under normoxic conditions, GC7 induced a fall in oxygen consumption in either cells or whole animals. Our hypothesis is that this fall in oxygen consumption is a consequence of the downregulation of mitochondrial complexes induced by inhibition of eIF5A hypusination. The mitochondrial potential falls down to a nonlethal level that is not associated with an overexpression of uncoupling proteins but rather, is associated with a subexpression of mitochondrial complexes. This result is consistent with previous findings showing that the hypusinated form of eIF5A interacts specifically with a small set of mRNAs, including the NADH dehydrogenase (complex 1) mRNA,[25] and influences translation of these proteins. This slowdown in mitochondrial activity is compensated by a metabolic shift toward anaerobic glycolysis to maintain the energetic status of the cells.

Classically, anoxic conditions favor the generation of deleterious oxygen reactive species,[30] and the prevention of ROS generation along an ischemic stress is one of the keys allowing the organ to survive to oxygen deprivation. One of the main consequences of this mitochondrial silencing is the absence of ROS production after the cells are submitted to anoxia, preventing them from death. Thus, GC7 seems to act as an agent of preconditioning to anoxic conditions through an HIF-independent pathway. AKI is currently a great challenge to overcome in clinical practice,[31] and the prevention of kidney dysfunction progression remains a critical point. Therefore, the search for safe and effective agents to ameliorate ischemia-reperfusion injury is of clinical relevance. The data that we obtained clearly show the protective effect of GC7 against the harmful effect of AKI. However, we have to

GC7-treated group (GC7). The brush border membrane morphology appeared preserved in GC7-treated animals. Scale bars, 0.5 μm. (E–G) Histograms representative of the TUNEL labeling (apoptotic cells), CellROX staining (oxidative stress), and 4-HNE labeling (lipid peroxidation) performed on kidney biopsies 30 minutes after reperfusion. Values are expressed in percentages of positive pixels for each probe compared with DAPI labeling. (H) Representative images for each group showing staining for fibrosis (Sirius red staining). Original magnification, ×100. (I) Fibrosis expressed as percentage of Sirius red staining by field. (J and K) Representative Western blots of PAI-1 (tPA inhibitor), tPA, and CTGF and quantitative analyses by densitometry of blots. Values are means±SEM of three animals per groups (*n*=3). *$P<0.50$, ANOVA and Tukey–Kramer multiple comparison post–test.

consider the negative results obtained in an attempt to protect kidney functions when GC7 is applied in a post-treatment protocol. This limits the use of GC7 in a pretreatment way. Hopefully, this is highly pertinent in the transplantation context, in which pretreatment can be scheduled. Over the past 50 years, kidney transplantation has become an established worldwide practice, bringing immense benefits to hundreds of thousands of patients. Organ transplantation is now the most cost–effective treatment for end stage renal failure. However, this success has led to an organ shortage crisis, and only one quarter of patients on the waiting list have access to organ transplantation. This state changed the donor demography, with the increased use of organs from extended criteria donors and deceased after circulatory death donors with important comorbidity factors.[32] These organs are more sensitive to the ischemia–reperfusion injury, which has a critical influence on graft dysfunctions. Kidneys from deceased after circulatory death donors are correlated with higher levels of delayed graft function and primary nonfunction.[33] This new donor demography pushes the community to investigate new conditioning methods to improve graft quality. In this context, proper donor or recipient management protocols including the use of innovative drugs, such as GC7, are of outmost importance. It is now shown that the intensity of ischemia-reperfusion injury very strongly correlates with delayed graft function, chronic graft dysfunction, and late graft loss,[34] and our data bring evidence that GC7 greatly enhanced the functional recovery of kidney after transplantation. From a more general point of view, this study provides an experimentally driven preclinical rationale for a new mechanistic–based pharmacologic therapy suitable for testing protection against ischemic injury.

CONCISE METHODS

GC7 Synthesis

GC7 was synthesized by AtlanChim Pharma (Saint-Herblain, France) according to the methods described by Jasiulionis *et al.*[35] The molecular structure and purity of the product were evaluated using NMR and mass spectrometry.

Cell Culture and Experimental Conditions

Renal PCT cells were obtained from primary cultures of murine proximal tubule segments, immortalized with pSV3neo vector, and cultured as previously described.[36,37] Cultures were classically maintained in a 5% CO_2 and 95% air water–saturated atmosphere. Hypoxic or anoxic conditions were obtained by maintaining the cell culture at 37°C in a sealed Bug-Box Anaerobic Workstation (Ruskin Technologies).

Silencing of DHPS and DOHH Proteins

In total, 150,000 PCT cells were cultured on petri dishes and then, transfected 24 hours later with 50 nM either DHPS or DOHH pool siRNAs (Sigma MISSIONesiRNA Targeting Mouse Dhps or Dohh: EMU150671 and EMU093741, respectively; Sigma-Aldrich, St. Louis, MO) using Lipofectamine 3000 Transfection Reagent (Invitrogen, Carlsbad, CA).

Cell Viability/Cytotoxicity Assay, Measurement of ROS Levels, and Mitochondrial Potential Measurements

The Fluorescent LIVE/DEAD Cell Viability/Cytotoxicity Assay Kit (Invitrogen) was used on PCT cells (24-well plates) according to the manufacturer's protocol. Fluorescent micrographs were recorded using an observer D1 microscope (Carl Zeiss GmbH, Jena, Germany). Fluorescent DAPI (Live Science) labeling was also used to estimate the number of cells in each field.

Intracellular oxidative stress (*i.e.*, ROS production) was measured using the fluorescent probe 5(and 6)-carboxy-2′,7′-dichlorodihydrofluorescein diacetate (Molecular Probes) according to the protocol described by L'Hoste *et al.*[37]

For measurement of mitochondrial membrane potentials ($\Delta\Psi_m$), cells were collected by trypsinization (0.05% trypsin and 0.53 mM EDTA) and loaded with 50 nM TMRE. The fluorescence intensity was determined at 488 nm excitation and 564–606 nm emission by flow cytometry (FACSCalibur; Becton Dickinson, San Diego, CA). $\Delta\Psi_m$ was also quantified in intact cultured cells using a fluorescent mitochondrial potential reporter (MitoTracker Red FM; Invitrogen). Confluent cultured cell monolayers were incubated with MitoTracker-Red FM (30–40 minutes; 1 μM), and fluorescence was quantified at 640 nm using a plate reader.

The carbocyanine–based fluorescent probe (MitoTracker Green FM; Invitrogen) and Mito DS Red Vector were used according to the manufacturer's protocol.

Oxygen Consumption

Adult male C57/Bl6 mice (Janvier-Europe) weighing 24±2 g received daily intraperitoneal injections of 0.9% control saline or GC7 (3 mg/kg in saline solution) for 3 days. For oxygen consumption, the nontreated or GC7-treated mice were maintained in a container (600 cm^3). After a short period of adaptation (30 minutes), the container was sealed, and the internal O_2 concentration was measured over a period of 40 minutes with an oxymeter (OXYBABY, Witt, Germany). To scavenge the toxic CO_2 expired by the animals, a solution of saturated barium hydroxide (50 ml at 37 g/L) was added to the container.

Western Blotting Analyses

Protein expression was analyzed by Western blotting analysis using the following antibodies: total eIF5A (1:2500; Abcam, Inc., Cambridge, MA), hypusinated form of eIF5A (1:200), Mitoprofile membrane integrity cocktail (MS620; Mitosciences), Mitoprofile total OXPHOS cocktail (MS601; Mitosciences), tubulin (1:5000; Sigma-Aldrich), and β-actin (1:10,000; Sigma-Aldrich). Equivalent amounts of protein were separated by SDS-PAGE on 8%–17.5% acrylamide gels and then, electrophoretically transferred to Hybond-C Extra Membrane (Amersham). Proteins were detected using HRP–labeled secondary antibodies and the Amersham ECL System. Band intensity was quantified by densitometric analysis (Fusion FX7, Vilbert-Lourmat, France).

Measurement of Cell Metabolism Parameters

Oxygen consumption was measured with a Clark Electrode (polarometric technique; YSI53) in a closed chamber (2 ml) and monitored using a Powerlab 8/35 Acquisition System (AD Instrument). The cell protein content in each experimental condition was quantified using a colorimetric assay kit (DC Protein Assay; Bio-Rad, Hercules, CA). The

glucose consumption was determined by quantifying the difference between the DMEM/F12 medium concentration measured at the beginning of the experiment and the residual glucose concentration measured at the end of the experiment using a colorimetric kit (Randox Kit; Randox Laboratories, Crumlin, United Kingdom). Measurement of cellular ATP content was performed using a luciferin/luciferase assay kit (ATPlite; PerkinElmer, Waltham, MA). The bioenergetic profile was established using a Seahorse XF96 Extracellular Flux Analyzer from Seahorse Bioscience (North Billerica, MA). Enzymatic spectrophotometric measurements of the OXPHOS respiratory chain complexes 1–5 were performed at 37°C on PCT cells according to standard procedures.[38] Proteins were measured according to Bradford microassays, and results were expressed as nanomoles per minute per milligram proteins.

Quantitative RT-PCR Analyses

Reverse transcription was performed using 2 μg RNA samples, M-MLV-RT (Promega, Madison, WI), and random primers (250 ng/μl; Roche Diagnostics, Indianapolis, IN). Preliminary to reaction, genomic DNA contaminant was eliminated by DNAse RQ1 (Promega) in presence of RNAsin (Promega). Primer sequences were designed using Primer Express software (Applied Biosystems, Foster City, CA) and tested for their specificity, efficiency, reproducibility, and dynamic range. For quantitative PCR, final reaction volume was 20 μl using SYBR Green Master Mix (Eurogentec, Angers, France) and 100 nM primers. Assays were run on an ABI Prism 7700 Real-Time PCR Machine (PerkinElmer). The expression of selected genes was quantified by the comparative ΔCt method using *36B4*, *β-actin*, *hprt1*, and *gapdh* as reference genes. Primer sequences were ucp2-s: AGGCCATAGACCTACAGAAGACAAG; ucp2-as: CCCCGGTTCAGAGCATGT; ucp3-s: GCTGGAGTCTCACCTGTTTACTGA; ucp3-as: ACAGAAGCCAGCTCCAAAGG; 36b4-s: TCCAGGCTTTGGGCATCA; 36b4-as: CTTTATCAGCTGCACATCACTCAGA; hprt-s: GCTGGTGAAAAGGACCTCT; hprt-as: CACAGGACTAGAACACCTGC; gapdh-s: GGCATTGTGGAAGGGCTCATGACGA; gapdh-as: TAGCCGTATTCATTGTCATACCAGG; β-actin-s: AGATCATGTTTGAGACCTTC; and β-actin-as: GTAGTTTCATGGATGCCACA.

In Vivo Ischemia-Reperfusion Protocol in Rat

All animal procedures were carried out in accordance with the French legislation for animal care and experimentation (C06–101). Adult female Wistar rats (190–240 g; 7–8 weeks old) received daily intraperitoneal injections for 3 days with 0.9% control saline or GC7 (3 mg/kg in saline solution). On day 4, rats were anesthetized with isoflurane. Using a left flank incision, the left renal artery was prepared and held with a vascular clamp for 40 minutes. The kidney was then observed for 1 minute after removal of the clamp to assess reperfusion, and the incision was sutured. Sham-operated animals were subjected to left flank incisions only. The contralateral right kidney was left untouched and served as an internal control. Twenty-four hours postsurgery, independent renal clearances of the left ischemic and right nonischemic kidneys were performed.[39] Urine was collected separately from each kidney, and the FEs of glucose, Na^+, and phosphate ions were determined using the hexokinase method (Colorimetric Kit; Randox Laboratories), flame atomic absorption spectrometry, and anion exchange chromatography (Dionex AS50; AS11 column), respectively. NGAL measurements were performed using a commercial NGAL kit (Bioporto) and are expressed as urinary NGAL-to-creatinine ratios to compensate for urinary dilution/concentration.

Porcine Kidney Autotransplantation

Surgical protocols were performed in accordance with the Animal Research: Reporting of In Vivo Experiments guidelines, the guidelines of the French Ministries of Agriculture and Research, and those of the Poitou-Charentes ethical committee for the use and care of laboratory animals (protocol number CE2012–4). We used 3-month-old large white pigs weighting 40±4 kg (MOPICT IBiSA Plateforme; INRA Magneraud, Surgeres, France). We intravenously infused GC7 (3 mg/kg) 24 and 3 hours before warm ischemia realized by renal pedicle clamping, and then, we removed the kidney and preserved it for 24 hours in University of Wisconsin solution at 4°C; then, we transplanted the kidney graft in the same animal after a contralateral nephrectomy, and the pig was followed up for 3 months. This warm ischemia associated with a cold storage mimicked the lesions observed in the deceased after cardiac death donor. We used n=3 per group determined by statistical covariance analysis, with creatininemia at day 3 post-transplantation as principal evaluation criteria, bilateral hypothesis, 5% α-risk, and 80%power. This choice is also adherent with the experimental animal use legislation and the need to reduce animal number. Plasma and urine were collected, and creatininemia, plasma aspartate aminoransferase, plasma alanine aminopeptidase, sodium FE, and osmolarity plasma/urine were measured with a Cobas Bioanalyser (Roche Diagnostics). Renal cortex tissue biopsies sampling was performed 30 minutes postreperfusion for evaluation of morphologic, apoptosis, and oxidative stress injuries. Renal biopsies were processed for transmission electron microscopy as previously described.[40] Biopsies were fixed in 3% glutaraldehyde, washed, and postfixed in 1% osmium tetroxide. Then, they were dehydrated in acetone and embedded in araldite. Ultrathin sections were cut and stained with uranyl acetate and lead citrate and examined under an electron microscope (JEOL 1010; JEOL, Tokyo, Japan). Histochemical and immunohistochemical studies to quantify the apoptotic cells were performed with a TUNEL kit (DeadEnd Fluorometric TUNEL System; Promega), and those to determine the oxidative stress were performed with the CellROX staining (CellROX Green Reagent; Thermo Fisher Scientific, Vernon Hills, IL) and the antibody against 4-HNE (ab5605; EMD Millipore, Billerica, MA). Renal tissue sampling was performed 3 months postreperfusion for histologic fibrosis evaluation (red Sirius staining) and Western blot analysis to measured expressions of tPA, PAI-1, and CTGF proteins. Red Sirius staining quantification was performed by quantifying the percentage of staining by field (Visilog 6.9 software). Western blotting was carried out using specific antibodies against PAI-1 (612024; BD Transduction, Le Pont de Claix, France), tPA (SC-15346; Santa Cruz Biotechnology, Santa Cruz, CA), and CTGF (5553R-100; BioVision Cliniscience, Nanterre, France).

ACKNOWLEDGMENTS

This work was supported by grant ANR-08-GENO-022 from the Agence Nationale de la Recherche, grant DPM 20121125559 from the Fondation pour la recherche médicale (FRM), and a grant from

the Société d'Accélération de Transfert de Technologie. N.M. was funded by FRM predoctoral fellowship FDT 20140931067.

DISCLOSURES

None.

REFERENCES

1. Scheper GC, van der Knaap MS, Proud CG: Translation matters: Protein synthesis defects in inherited disease. *Nat Rev Genet* 8: 711–723, 2007
2. Fähling M: Surviving hypoxia by modulation of mRNA translation rate. *J Cell Mol Med* 13: 2770–2779, 2009
3. Wolff EC, Kang KR, Kim YS, Park MH: Posttranslational synthesis of hypusine: Evolutionary progression and specificity of the hypusine modification. *Amino Acids* 33: 341–350, 2007
4. Park MH, Nishimura K, Zanelli CF, Valentini SR: Functional significance of eIF5A and its hypusine modification in eukaryotes. *Amino Acids* 38: 491–500, 2010
5. Cooper HL, Park MH, Folk JE, Safer B, Braverman R: Identification of the hypusine-containing protein hy+ as translation initiation factor eIF-4D. *Proc Natl Acad Sci U S A* 80: 1854–1857, 1983
6. Park MH: The post-translational synthesis of a polyamine-derived amino acid, hypusine, in the eukaryotic translation initiation factor 5A (eIF5A). *J Biochem* 139: 161–169, 2006
7. Kemper WM, Merrick WC, Redfield B, Liu CK, Weissbach H: Purification and properties of rabbit reticulocyte elongation factor 1. *Arch Biochem Biophys* 174: 603–612, 1976
8. Zanelli CF, Valentini SR: Is there a role for eIF5A in translation? *Amino Acids* 33: 351–358, 2007
9. Park MH, Joe YA, Kang KR: Deoxyhypusine synthase activity is essential for cell viability in the yeast Saccharomyces cerevisiae. *J Biol Chem* 273: 1677–1683, 1998
10. Caraglia M, Marra M, Giuberti G, D'Alessandro AM, Budillon A, del Prete S, Lentini A, Beninati S, Abbruzzese A: The role of eukaryotic initiation factor 5A in the control of cell proliferation and apoptosis. *Amino Acids* 20: 91–104, 2001
11. Kaiser A: Translational control of eIF5A in various diseases. *Amino Acids* 42: 679–684, 2012
12. Vigne P, Frelin C: The role of polyamines in protein-dependent hypoxic tolerance of Drosophila. *BMC Physiol* 8: 22, 2008
13. Kato J, Nakayama M, Zhu W-J, Yokoo T, Ito S: Ischemia/reperfusion of unilateral kidney exaggerates aging-induced damage to the heart and contralateral kidney. *Nephron Exp Nephrol* 126: 183–190, 2014
14. Lee YB, Folk JE: Branched-chain and unsaturated 1,7-diaminoheptane derivatives as deoxyhypusine synthase inhibitors. *Bioorg Med Chem* 6: 253–270, 1998
15. Duranton C, Rubera I, Cougnon M, Melis N, Chargui A, Mograbi B, Tauc M: CFTR is involved in the fine tuning of intracellular redox status: Physiological implications in cystic fibrosis. *Am J Pathol* 181: 1367–1377, 2012
16. Brahimi-Horn MC, Bellot G, Pouysségur J: Hypoxia and energetic tumour metabolism. *Curr Opin Genet Dev* 21: 67–72, 2011
17. Papandreou I, Cairns RA, Fontana L, Lim AL, Denko NC: HIF-1 mediates adaptation to hypoxia by actively downregulating mitochondrial oxygen consumption. *Cell Metab* 3: 187–197, 2006
18. Buravkov SV, Pogodina MV, Buravkova LB: Comparison of mitochondrial fluorescent dyes in stromal cells. *Bull Exp Biol Med* 157: 654–658, 2014
19. Barratt TM, Walser M: Extracellular fluid in individual tissues and in whole animals: The distribution of radiosulfate and radiobromide. *J Clin Invest* 48: 56–66, 1969
20. Haase M, Bellomo R, Devarajan P, Schlattmann P, Haase-Fielitz A; NGAL Meta-analysis Investigator Group: Accuracy of neutrophil gelatinase-associated lipocalin (NGAL) in diagnosis and prognosis in acute kidney injury: A systematic review and meta-analysis. *Am J Kidney Dis* 54: 1012–1024, 2009
21. Kwon TH, Frøkiaer J, Han JS, Knepper MA, Nielsen S: Decreased abundance of major Na(+) transporters in kidneys of rats with ischemia-induced acute renal failure. *Am J Physiol Renal Physiol* 278: F925–F939, 2000
22. Favreau F, Thuillier R, Cau J, Milin S, Manguy E, Mauco G, Zhu X, Lerman LO, Hauet T: Anti-thrombin therapy during warm ischemia and cold preservation prevents chronic kidney graft fibrosis in a DCD model. *Am J Transplant* 10: 30–39, 2010
23. Małgorzewicz S, Skrzypczak-Jankun E, Jankun J: Plasminogen activator inhibitor-1 in kidney pathology (Review). *Int J Mol Med* 31: 503–510, 2013
24. Brigstock DR: Connective tissue growth factor (CCN2, CTGF) and organ fibrosis: Lessons from transgenic animals. *J Cell Commun Signal* 4: 1–4, 2010
25. Xu A, Jao DL, Chen KY: Identification of mRNA that binds to eukaryotic initiation factor 5A by affinity co-purification and differential display. *Biochem J* 384: 585–590, 2004
26. Saini P, Eyler DE, Green R, Dever TE: Hypusine-containing protein eIF5A promotes translation elongation. *Nature* 459: 118–121, 2009
27. Maier B, Ogihara T, Trace AP, Tersey SA, Robbins RD, Chakrabarti SK, Nunemaker CS, Stull ND, Taylor CA, Thompson JE, Dondero RS, Lewis EC, Dinarello CA, Nadler JL, Mirmira RG: The unique hypusine modification of eIF5A promotes islet beta cell inflammation and dysfunction in mice. *J Clin Invest* 120: 2156–2170, 2010
28. Robbins RD, Tersey SA, Ogihara T, Gupta D, Farb TB, Ficorilli J, Bokvist K, Maier B, Mirmira RG: Inhibition of deoxyhypusine synthase enhances islet beta cell function and survival in the setting of endoplasmic reticulum stress and type 2 diabetes. *J Biol Chem* 285: 39943–39952, 2010
29. Legrand M, Mik EG, Johannes T, Payen D, Ince C: Renal hypoxia and dysoxia after reperfusion of the ischemic kidney. *Mol Med* 14: 502–516, 2008
30. Nath KA, Norby SM: Reactive oxygen species and acute renal failure. *Am J Med* 109: 665–678, 2000
31. Leite TT, Macedo E, Pereira SM, Bandeira SR, Pontes PH, Garcia AS, Militão FR, Sobrinho IM, Assunção LM, Libório AB: Timing of renal replacement therapy initiation by AKIN classification system. *Crit Care* 17: R62, 2013
32. Brook NR, Nicholson ML: Kidney transplantation from non heart-beating donors. *Surgeon* 1: 311–322, 2003
33. Troppmann C, Gillingham KJ, Benedetti E, Almond PS, Gruessner RW, Najarian JS, Matas AJ: Delayed graft function, acute rejection, and outcome after cadaver renal transplantation. The multivariate analysis. *Transplantation* 59: 962–968, 1995
34. Perico N, Cattaneo D, Sayegh MH, Remuzzi G: Delayed graft function in kidney transplantation. *Lancet* 364: 1814–1827, 2004
35. Jasiulionis MG, Luchessi AD, Moreira AG, Souza PP, Suenaga AP, Correa M, Costa CA, Curi R, Costa-Neto CM: Inhibition of eukaryotic translation initiation factor 5A (eIF5A) hypusination impairs melanoma growth. *Cell Biochem Funct* 25: 109–114, 2007
36. L'Hoste S, Poet M, Duranton C, Belfodil R, é Barriere H, Rubera I, Tauc M, Poujeol C, Barhanin J, Poujeol P: Role of TASK2 in the control of apoptotic volume decrease in proximal kidney cells. *J Biol Chem* 282: 36692–36703, 2007
37. L'hoste S, Chargui A, Belfodil R, Duranton C, Rubera I, Mograbi B, Poujeol C, Tauc M, Poujeol P: CFTR mediates cadmium-induced apoptosis through modulation of ROS level in mouse proximal tubule cells. *Free Radic Biol Med* 46: 1017–1031, 2009
38. Rustin P, Chretien D, Bourgeron T, Gérard B, Rötig A, Saudubray JM, Munnich A: Biochemical and molecular investigations in respiratory chain deficiencies. *Clin Chim Acta* 228: 35–51, 1994
39. Barbier O, Jacquillet G, Tauc M, Poujeol P, Cougnon M: Acute study of interaction among cadmium, calcium, and zinc transport along the rat nephron in vivo. *Am J Physiol Renal Physiol* 287: F1067–F1075, 2004
40. Goujon JM, Hauet T, Menet E, Levillain P, Babin P, Carretier M: Histological evaluation of proximal tubule cell injury in isolated perfused pig kidneys exposed to cold ischemia. *J Surg Res* 82: 228–233, 1999

This article contains supplemental material online at http://jasn.asnjournals.org/lookup/suppl/doi:10.1681/ASN.2016010012/-/DCSupplemental.